
Auto-Encoding Adversarial Imitation Learning

Kaifeng Zhang¹ Rui Zhao² Ziming Zhang³ and Yang Gao^{1,4}

¹Shanghai Qi Zhi Institute ²Tencent AI Lab

³Worcester Polytechnic Institute ⁴Tsinghua Univeristy

Abstract

Reinforcement learning (RL) provides a powerful framework for decision-making, but its application in practice often requires a carefully designed reward function. Adversarial Imitation Learning (AIL) sheds light on automatic policy acquisition without access to the reward signal from the environment. In this work, we propose Auto-Encoding Adversarial Imitation Learning (AEAIL), a robust and scalable AIL framework. To induce expert policies from demonstrations, AEAIL utilizes the reconstruction error of an auto-encoder as a reward signal, which provides more information for optimizing policies than the prior discriminator-based ones. Subsequently, we use the derived objective functions to train the auto-encoder and the agent policy. Experiments show that our AEAIL performs superior compared to state-of-the-art methods in the MuJoCo environments. More importantly, AEAIL shows much better robustness when the expert demonstrations are noisy. Specifically, our method achieves 16.4% and 47.2% relative improvement overall compared to the best baseline FAIRL and PWIL on clean and noisy expert data, respectively. Video results, open-source code and dataset are available in <https://sites.google.com/view/auto-encoding-imitation>.

1 Introduction

Reinforcement learning (RL) provides a powerful framework for automated decision-making. However, RL still requires significantly engineered reward functions for good practical performance. Imitation learning offers the instruments to learn policies directly from the demonstrations, without an explicit reward function. It enables the agents to learn to solve tasks from expert demonstrations, such as helicopter control [5, 3, 34, 1, 2], robot navigation [39, 4, 50, 49], and building controls [7].

The goal of imitation learning is to induce the expert policies from expert demonstrations without access to the reward signal from the environment. We divide these methods into two broad categories: Behavioral Cloning (BC) and Inverse Reinforcement Learning (IRL). Among IRL, adversarial imitation learning (AIL) induces expert policies by minimizing the distribution distance between expert samples and agent policy rollouts. Prior AIL methods model the reward function as a discriminator to learn the mapping from the state-action pair to a scalar value, i.e., reward [25]. However, the discriminator in the AIL framework would easily find the differences between expert samples and agent-generated ones, even though some differences are minor. Therefore, the discriminator-based reward function would yield a sparse reward signal to the agent. Consequently, how to make AIL robust and efficient to use is still subject to research.

To the best of our knowledge, our AEAIL is the first instance of formulating the reward function as an auto-encoder. It enables the capability to learn the full-scale differences between expert and generated policies. Thus, the derived denser reward signal would guide the agent policy to be better [35]. Specifically, we use the reconstruction error of the auto-encoder to compute the rewards for the agent. This reward signal ignores some minor differences between expert and generated samples with small differences on the value of reconstruction error. Therefore, it provides a much better reward to the agent policy in realistic settings.

Our contributions are three-fold:

- We propose the Auto-Encoding Adversarial Imitation Learning (AEAIL) architecture. It models the reward function as the reconstruction error of an auto-encoder. It focuses on the full-scale differences between the expert and generated samples, and less susceptible to the discriminator attending to minor differences.
- Experiments show that our proposed AEAIL achieves the best overall performance on many environments compared to other state-of-the-art baselines.
- Empirically, we justify that our AEAIL works under a wide range of distribution divergences and auto-encoders. And the major contributing factor of our method is the encoding-decoding process rather than the specific divergence or auto-encoder.

2 Related work

2.1 Imitation learning

Discriminator based IRL IRL methods such as GAIL, AIRL, DAC, f -GAIL, EAIRL, FAIRL [25, 17, 31, 47, 38, 19] formulates the learned reward function as a discriminator that learns to differentiate expert transitions from non-expert ones. Among these methods, GAIL [25] considers the Jensen-Shannon divergence, while AIRL [17] considers the Kullback-Leibler (KL) divergence. DAC [31] extends GAIL to the off-policy setting and significantly improves the sample efficiency of adversarial imitation learning. Furthermore, f -divergence is utilized in f -GAIL [47], which is considered improving sample-efficiency. Recently, FAIRL utilizes the forward KL divergence [19] and achieves great performance, but it is still not robust and efficient enough. These methods rely heavily on a carefully tuned discriminator based reward function. It might focus on the minor differences between the expert and the generated samples and thus gives a sparse reward signal to the agent. In comparison, our auto-encoder-based reward function learns the full-scale differences between the expert and generated samples. It provides a denser reward signal.

Imitation with Imperfection The robustness of adversarial imitation learning is questionable with imperfection in observations [43, 9], actions, transition models [18, 13], expert demonstrations [12, 42, 27] and their combination [28]. Prior robust imitation learning methods require the demonstrations to be annotated with confidence scores [46, 12, 22]. However, these annotations are rather expensive. Compared to this, our auto-encoder-based reward function won't easily overfit to the noisy feature. Therefore, our AEAIL is relatively straightforward and robust to the noisy expert data and does not require any annotated data.

Hand-Crafted Reward-based IRL Another category of IRL uses a hand-crafted similarity function to estimate the rewards [11, 30, 37]. The idea of these methods is still inducing the expert policy by minimizing the distance between the state action distributions of the expert and sampled trajectories. To the best of our knowledge, the best method in this category is Primal Wasserstein Imitation Learning (PWIL) [15], which utilizes the upper bound of its primal form as the optimization objective. The advantage of these methods is that they are relatively more robust and less demonstration dependent than AIL methods. However, the performance of these methods heavily depends on the similarity measurement, and therefore, it varies greatly on different tasks. Compared to PWIL, our method achieves superior performance via automatically acquiring a similarity measurement.

2.2 Auto-Encoding based GANs

Auto-encoders have been successfully applied to improve the training stability and modes capturing in GANs. We classify Auto-encoding based GANs into three categories: (1) utilizing an auto-encoder as the discriminator such as energy-based GANs [48] and boundary-equilibrium GANs [10]; (2) using a denoising auto-encoder to derive an auxiliary loss for the generator [45]; (3) combining variational auto-encoder and GANs to generate both vivid and diverse samples by balancing the objective of reconstructing the training data and confusing the discriminator [32]. Our method AEAIL takes inspirations from EBGAN [48], utilizing the auto-encoder as the reward function.

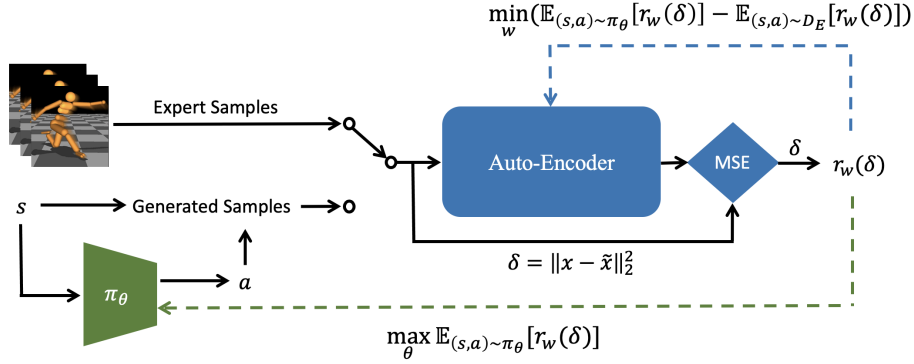


Figure 1: Training framework of our AEAIL. The auto-encoder computes the reconstruction error for these two mini-batches of data examples and optimizes the derived objectives. Therefore, a surrogate reward function $r_w(\delta)$ provides the signal to the agent. The agent can induce the expert policies by iteratively training the auto-encoder and the agent policy.

3 Background

Inverse Reinforcement Learning (IRL) IRL extracts the policy towards mimicking expert behaviors with the help of a learned reward function. On the other hand, AIL directly induces the expert policies by minimizing the distribution distance between expert demonstrations and agent-generated samples.

Adversarial Imitation Learning (AIL) Assume that we are given a set of expert demonstrations, AIL involves a discriminator which tries to distinguish the expert and policy generated samples and a policy that is optimized to confuse the discriminator accordingly. Ideally, the rollouts from the agent will be indistinguishable from the expert demonstrations in the end. The discriminator cannot classify the expert samples and policy-generated ones any more at the end of the training. Consequently, this kind of discriminator-based reward function can be seen as a pseudo-reward signal, which is only used for optimizing policies during training.

Wasserstein Divergence One popular distribution divergence for measuring the distance between policy samples and expert samples is the Wasserstein divergence [6]:

$$d(p, q) = \sup_{\phi} \mathbb{E}_{x \sim p} [\phi(x)] - \mathbb{E}_{y \sim q} [\phi(y)], \quad (1)$$

where p and q are two probability distributions. Equation 1 measures the distance between these two distributions. Intuitively, we can view it as the minimum cost of turning the piles from distribution p into the holes in distribution q .

Wasserstein GAIL (WGAIL) WGAIL [6, 25] combines the Wasserstein distance and GAIL [25] as optimizing:

$$\min_{r \in \mathcal{R}} \left(\max_{\pi \in \Pi} \mathbb{E}_{\pi} [r(s, a)] - \mathbb{E}_{\pi_E} [r(s, a)] \right) \quad (2)$$

Equation 2 looks for a discriminator-based reward function $r(s, a)$ that assigns high values to the expert policy and low values to other policies. Therefore, it allows the expert policy to be found with a certain reinforcement learning procedure:

$$\text{RL}(r) = \arg \max_{\pi \in \Pi} \mathbb{E}_{\pi} [r(s, a)] \quad (3)$$

WGAIL will induce the expert policy via iteratively optimizing the RL agent policy with reward $r(s, a)$ and update the discriminator-based pseudo-reward signal (Implementation details see in Appendix A.2.4).

4 Methodology

4.1 Overview

The reward function in GAIL is a discriminator, which attempts to assign high values to the regions near the expert demonstrations and assign low values to the other areas. However, the discriminator

would easily overfit to the minor differences between expert data and policy-generated samples. Consider the CartPole balancing task, the state of the environment is a feature consisting of position, angle, angle’s rate, and cart velocity while the action is moving left or right. Here, we assume that all the expert states’ velocity is 2, for example. When the generated states’ velocity is 1.9, and other dimensions of state-action pair are the same as the expert’s, the discriminator of GAIL would still give a low reward on these generated state-action samples. However, the policy rollouts may perform very well towards mimicking the expert’s behaviors. In other words, the reward function in GAIL on this example overfits to the minor differences between the expert and the sampled data and leads the policy to miss the underlying goal of the expert.

In this paper, we propose an auto-encoder-based reward function for adversarial imitation learning. It utilizes the reconstruction error of the state action pairs to yield a much denser reward signal. Furthermore, the reconstruction error based reward signal significantly retains the information of state-action pairs rather than focusing on the minor differences. Therefore, this reward signal wouldn’t lead to overconfidence in distinguishing the expert and the generated samples. Recall the CartPole example, the mean square error between states’ velocity 1.9 and 2 is very small. And it could still feed a good reward to the agent under this situation. Therefore, the reconstruction error based reward signal can better focus on the full-scale differences between the expert and generated state action pairs rather than the minor parts. Thus, this kind of reward signal would guide the policy to better mimic expert behaviors.

4.2 Our method

Our approach is to minimize the distance between the state action distribution of the policy π_θ and that of the expert demonstrations D_E . The distance we used in our method is the Wasserstein distance [6]:

$$d(\pi_E, \pi_\theta) = \sup_{r_w} \mathbb{E}_{\pi_E}[r_w(s, a)] - \mathbb{E}_{\pi_\theta}[r_w(s, a)], \quad (4)$$

where the reward function network’s parameters are denoted as w and the policy network’s parameters are represented as θ . We use the full class of neural networks. We do not use any weight clipping or gradient penalty for Lipschitz constraint. Minimizing this distance will induce the expert policy from expert demonstrations. Therefore, the optimization of the policy π_θ and the reward function $r_w(s, a)$ forms a bi-level optimization problem, which can be formally defined as:

$$\min_{\pi_\theta} \max_{r_w} (\mathbb{E}_{(s,a) \sim D_E}[r_w(s, a)] - \mathbb{E}_{(s,a) \sim \pi_\theta}[r_w(s, a)]). \quad (5)$$

Optimizing Equation 5 leads to an adversarial formulation for imitation learning. The outer level minimization with respect to the policy leads to a learned policy that is close to the expert. The inner level maximization recovers a reward function that attributes higher values to regions close to the expert data and penalizes all other areas.

In prior AIL methods, such as WGAIL [6, 25], the pseudo-reward function for optimizing the agent policy is defined as:

$$r_w(s, a) = D_w(s, a), \quad (6)$$

where $D_w(s, a)$ is the output of the discriminator.

In our method, we use an auto-encoder based surrogate pseudo-reward function instead, which is defined as:

$$r_w(s, a) = 1/(1 + \text{AE}_w(s, a)), \quad (7)$$

where AE is the reconstruction error of an auto-encoder:

$$\text{AE}(x) = \|\text{Dec} \circ \text{Enc}(x) - x\|_2^2 \quad (8)$$

Here, x represents the state-action pairs. Equation 8 is the mean square error between the sampled state-action pairs and the reconstructed samples. This form of the reward signal uses the reconstruction error of an auto-encoder to score the state-action pairs in the trajectories. Equation 7 is a monotonically decreasing function over the reconstruction error of the auto-encoder. We give high rewards to the state-action pairs with low reconstruction errors of the auto-encoding process and vice versa. Section 4.1 motivates that this form of reward signal focuses more on the full-scale differences between the

expert and generated samples, and it won't easily overfit to the noise of the expert data. Therefore, it can more robustly guide the agent policy.

Training the auto-encoder is an adversarial process considering the objective 5, which is minimizing the reconstruction error for the expert samples while maximizing this error for generated samples. When combining Equation 5 and Equation 7, we can obtain the training objective for the auto-encoder as:

$$\begin{aligned}\mathcal{L} &= \mathbb{E}_{(s,a)\sim\pi_\theta}[r_w(s,a)] - \mathbb{E}_{(s,a)\sim D_E}[r_w(s,a)] \\ &= \mathbb{E}_{(s,a)\sim\pi_\theta}[1/(1 + \text{AE}_w(s,a))] - \\ &\quad \mathbb{E}_{(s,a)\sim D_E}[1/(1 + \text{AE}_w(s,a))].\end{aligned}\tag{9}$$

With this adversarial objective, the auto-encoder learns to maximize the full-scale differences between the expert and the generated samples. As a result, it gives the agent a denser reward signal. Furthermore, the agent can also be more robust when facing noisy expert data due to the robust auto-encoding objective.

Figure 1 depicts the architecture for AEAIL. The auto-encoder-based reward function takes either expert or the generated state-action pairs and estimates the reconstruction error based rewards accordingly. We iteratively optimize the auto-encoder and the agent policy under this adversarial training paradigm. Algorithm 1 in Appendix A.1 shows the pseudo-code for training AEAIL.

4.3 Theoretical convergence properties

Our AEAIL shares a similar theoretical framework with GAIL, where the auto-encoder based reward function can be seen as a generalized discriminator. [23] investigates the theoretical properties of GAIL. We make the same set of assumptions for our auto-encoder based reward function as these for the discriminator in GAIL [23]:

(i) the auto-encoder based reward function has bounded gradient, i.e., $\exists C_r \in \mathbb{R}$, such that

$$\|\nabla_w r_w\|_{\infty,2} := \sqrt{\sum_i \left\| \frac{\partial r_w}{\partial w_i} \right\|_{\infty}^2} \leq C_r$$

(ii) the auto-encoder based reward function has L-Lipschitz continuous gradient, i.e., $\exists L_r \in \mathbb{R}$, such that $\forall s \in \mathcal{S}, \forall a \in \mathcal{A}, \forall w_1, w_2 \in \mathcal{W}$, then:

$$\|\nabla_w r_{w_1}(s, a) - \nabla_w r_{w_2}(s, a)\|_2 \leq L_r \|w_1 - w_2\|_2$$

(iii) the distribution divergence is properly regularized to be strongly concave with respect to the reward function.

These conditions are assumptions for theoretical convenience since they don't always hold for a multi-layer neural network-based discriminator in GAIL or our proposed auto-encoder. When these assumptions hold, our AEAIL shares the same theoretical properties as GAIL: it converges globally.

5 Experiments

Environments: we conduct the experiments on six locomotion tasks with varying dynamics and difficulties: Swimmer-v2 [40], Hopper-v2 [33], Walker2d-v2 [40], HalfCheetah-v2 [24], Ant-v2 [41], and Humanoid-v2 [44].

Baselines: the baselines we choose for comparison includes: Behavior Cloning (BC) [16], GAIL [25], WGAIL [6, 25], FAIRL [19], and PWIL [15].

Implementation: experimental details, including the implementation and more results, are shown in Appendix A.2 to A.6. For a fair comparison, we use TRPO [40] as the policy search method for all the algorithms, which is implemented by OpenAI Baselines [16]. We also conduct experiments with the more advanced expert agent (D4PG) in Appendix A.7.

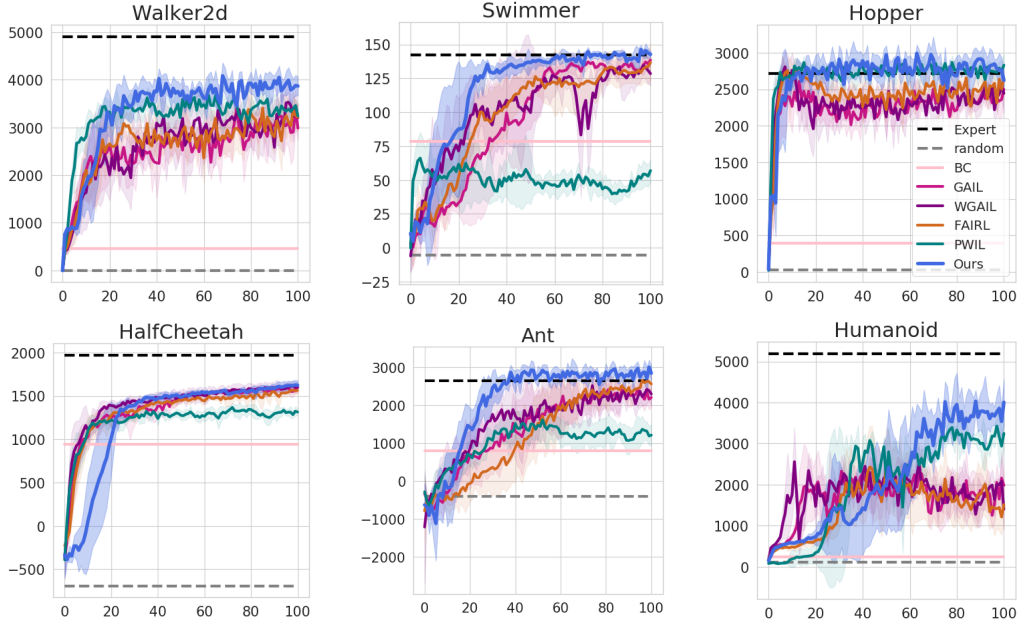


Figure 2: Mean and standard deviation return of the evaluation policy over 10 rollouts and 5 seeds, reported every 100k timesteps, which are learning from non-noisy expert demonstrations.

Table 1: Learned policy performance for different imitation learning algorithms on non-noisy expert data.

Task	Walker2d	Hopper	Swimmer	HalfCheetah	Ant	Humanoid
Expert	4904.2	2719.8	142.2	1969.2	2646.1	5187.9
Random	-0.6 ± 0.3	26 ± 4	-5 ± 14	-694 ± 108	-401 ± 233	110 ± 4
BC	460 ± 375	397 ± 436	78 ± 40	945 ± 161	808 ± 1844	238 ± 621
GAIL	2987 ± 256	2499 ± 66	138 ± 3	1597 ± 36	2207 ± 255	1981 ± 267
WGAIL	3204 ± 295	2443 ± 276	129 ± 9	1600 ± 66	2296 ± 295	1397 ± 502
FAIRL	3214 ± 291	2650 ± 102	137 ± 14	1563 ± 40	2563 ± 285	1513 ± 463
PWIL	3244 ± 224	2829 ± 144	57 ± 8	1314 ± 37	1216 ± 282	3246 ± 377
Ours	3870 ± 196	2621 ± 140	143 ± 3	1623 ± 52	2846 ± 204	4004 ± 570

5.1 Learning from expert demonstrations

To compare the performance of our proposed AEAIL and other baselines, we run the experiments on the expert dataset. We used the ground truth average return for evaluating different learned policies. Higher rewards indicate better mimicking expert behaviors.

Figure 2 depicts the training curves of ground truth rewards for different imitation learning algorithms, and Table 1 shows the final learned policy performance on MuJoCo tasks with ground truth episode return. Results show that GAIL, WGAIL, and FAIRL achieve comparable results, while WGAIL and FAIRL are a little better than GAIL comprehensively on these tasks but still not good enough. PWIL performs well on Walker2d, Hopper, and Humanoid tasks while poorly on other tasks. The performance of PWIL varies significantly on different tasks.

Our method’s overall scaled reward is about 0.910, whereas the best baseline is 0.781 for FAIRL. There is an about 16.4% relative improvement. Our method outperforms other state-of-the-art baselines on all locomotion tasks except for Hopper, where our approach doesn’t outperform PWIL and FAIRL. Here we would like to point out that our AEAIL has already achieved 97.3% of the expert performance on Hopper, which is very close to completely solving the task. We hypothesize that PWIL is better than ours because PWIL use a manual design of the distance metric, and that works well for low dimensional tasks such as Hopper.

Table 2: Learned policy performance for different imitation learning algorithms on noisy expert data.

Task	Walker2d	Hopper	Swimmer	HalfCheetah	Ant	Humanoid
BC	728 ± 835	196 ± 16	36 ± 2	898 ± 828	624 ± 1364	187 ± 5244
GAIL	1212 ± 235	1408 ± 266	108 ± 19	877 ± 107	1481 ± 903	940 ± 401
WGAIL	941 ± 384	1095 ± 406	96 ± 15	697 ± 212	1458 ± 360	1479 ± 540
FAIRL	1302 ± 554	1732 ± 328	106 ± 12	940 ± 98	-767 ± 518	1669 ± 511
PWIL	2958 ± 728	2700 ± 167	56 ± 5	1040 ± 22	-442 ± 739	3079 ± 354
Ours	3491 ± 369	2072 ± 327	110 ± 8	1487 ± 105	2622 ± 445	3666 ± 155

5.2 Learning from noisy expert demonstrations

Imitation with Noisy Expert To show the robustness of our proposed AEAIL, we further conduct experiments on noisy expert data. Table 2 shows the final learned policy performances on benchmarks. (For details and training curves see Appendix A.3). These results show that our method outperforms other state-of-the-art algorithms on all tasks except for Hopper, on which PWIL wins. Our AEAIL offers an excellent capability in learning from noisy expert data on these tasks. The overall scaled rewards for our AEAIL is 0.794, whereas the best baseline is 0.539 for PWIL on the noisy expert setting. There is an about 47.2% relative improvement. Other baselines including GAIL, WGAIL, and FAIRL, are very sensitive to the noisy expert. We also conduct experiments on another noisy expert with different noise magnitude in Appendix A.3. The performance shows that our AEAIL is consistently better than other baselines on different noise magnitudes.

Relative Improvements of AEAIL Figure 3 shows the relative improvement of overall scaled rewards for our AEAIL compared to GAIL on both clean and noisy expert data. The abscissa axis represents different tasks with the growth of task dimension, from Swimmer (dim=10) to Humanoid (dim=393). With the increasing task dimension, the relative improvement of our AEAIL shows an increasing trend. It indicates that our method has much more benefits when applied into high dimensional environments. At the same time, AEAIL achieves higher relative improvements on the noisy expert data setting than those on the non-noisy setting. We hypothesize that the discriminator in GAIL would focus much more on the minor differences between the expert and agent samples with the growth of task dimension. It is harder for GAIL to scale in higher dimensional tasks. On the other hand, our encoding-decoding process provides more information to the policy learning. Consequently, AEAIL scales relatively better than GAIL in higher dimensional tasks.

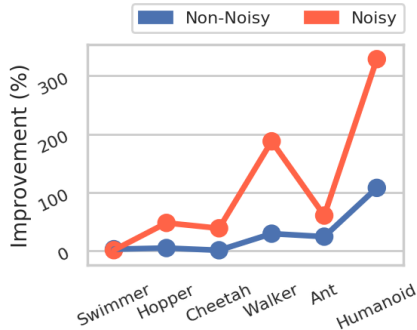


Figure 3: Relative improvement of our AEAIL compared to GAIL in different environments. Environments are sorted by the number of state-action dimensions.

Video Performance We also record a video¹ for the performance of different methods on both clean and noisy data. It shows that only our AEAIL can move forward as quickly as the expert from noisy expert data, while other baselines suffer from various types of failures.

5.3 Empirical analysis

A denser reward signal is beneficial for policy search [35, 26]. Section 4.1 motivates that our auto-encoder-based reward function focused on the full-scale differences between the expert and generated samples. Thus, it provides the agent with a denser reward signal than discriminator-based.

Question 1. *Is the auto-encoder-based reward signal denser than the discriminator-based one?*

¹Video results, code and data attached in supplementary materials.

To answer Question 1, we use the variance of learned rewards as a proxy for the denseness, which measures how frequently the rewards are far from zero. Note that the pseudo-rewards is never exactly zero but might be very close to zero. Thus, the denseness of reward is a generalization of the traditional definition. The higher variance of learned rewards means the reward signal can better score the performance of different state-action pairs, thus providing a denser reward signal to the agent policy. Specifically, we record the learned rewards for state-action pairs in each batch for policy optimization every iteration. Then, we compute the variance for this reward batch. Since the rewards of WGAIL and our AEAIL are on the same scale, a higher variance curve indicates it’s a denser reward signal.

Figure 4 shows the curve of variance of learned pseudo-rewards for generated samples in each batch for policy optimization, reported every 100 times policy optimization over 5 random seeds. Our AEAIL gets a much higher variance curve in the training process. It shows that our auto-encoder-based reward signal is denser than the discriminator-based one.

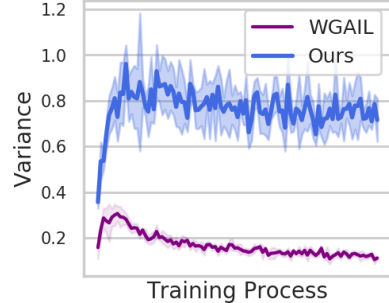


Figure 4: Variance of learned rewards for state-action pairs in each batch for training the agent-policy on Walker2d. y-label: variance of rewards; x-label: reported every 100 policy optimization.

5.4 Ablation study

Question 2. *What is the major contributing factor of our AEAIL? Could it be the specific W-distance metric?*

To analyze the major contributing factor of our AEAIL, we conduct an ablation study that replaces the Wasserstein distance to other distribution divergences. Comparable performances indicate that the major contributing factor is the encoding-decoding process rather than the specific distribution divergence. To justify this hypothesis, we formulate another form of surrogate reward function based on Jensen-Shannon divergence [21].

Jensen-Shannon divergence [21] is defined as:

$$\begin{aligned}
 \text{JS}(P_r, P_g) = & \mathbb{E}_{x \sim P_r} \left[\log \left(\frac{P_r(x)}{\frac{1}{2}(P_r(x) + P_g(x))} \right) \right] + \\
 & \mathbb{E}_{x \sim P_g} \left[\log \left(\frac{P_g(x)}{\frac{1}{2}(P_r(x) + P_g(x))} \right) \right]
 \end{aligned}
 \tag{10}$$

where P_r and P_g represent the expert data distribution and the agent-generated sample distribution accordingly.

Like the original W-distance based method, our JS-based variant induces the expert policy by minimizing the distribution distance between expert and generated samples. Specifically, we define that:

$$P_r(x) / (P_r(x) + P_g(x)) = \exp(-\text{AE}(x))
 \tag{11}$$

where $\text{AE}(x)$ is the same with Equation 8 in our original AEAIL. Minimizing Jensen-Shannon divergence assigns low mean square errors to the expert samples and high mean square errors to other regions. More details and full results, see in Appendix A.5.

Table 3 shows that our JS-based variant achieves 10.6% and 35.1% relative improvement compared to the best baseline FAIRL and PWIL on clean and noisy expert data, respectively. Similar to the original W-distance-based method, our JS-based variant also greatly improves the imitation performance on these benchmarks. The relative improvements are comparable between the two distance metrics. It indicates that

Table 3: Relative improvements for different variants of our AEAIL compared to the best baseline FAIRL and PWIL on clean and noisy data, respectively.

Improvements	Ours	Ours-JS	Ours-VAE
Clean Data	16.4%	10.6%	8.1%
Noisy Data	47.2%	35.1%	34.8%

the major contributing factor of our AEAIL is the encoding-decoding process. This also shows that AEAIL works not limited to a specific distance metric.

Question 3. *Is AEAIL limited to the specific type of auto-encoders? How about utilizing variational auto-encoders?*

To prove that our AEAIL is not sensitive to a specific type of auto-encoders, we conduct experiments by replacing the vanilla auto-encoder with the variational auto-encoder. If variational auto-encoder leads to similar performance on the benchmarks, it illustrates that AEAIL works under a wide range of different auto-encoders. We run the VAE-based variant on MuJoCo tasks under the same setting as the AE-based one.

The objective for training the VAE-based pseudo-reward function is:

$$\begin{aligned} \mathcal{L} = & \mathbb{E}_{(s,a) \sim D_E} [r_w(s, a) + D_{\text{KL}}(p(z|(s, a)), p_{\text{model}}(z))] \\ & - \mathbb{E}_{(s,a) \sim \pi_\theta} [r_w(s, a) + D_{\text{KL}}(p(z|(s, a)), p_{\text{model}}(z))] \end{aligned} \quad (12)$$

where the formulation of $r_w(s, a)$ is the same with our original AE-based one and z is the latent space representation. Intuitively, optimizing Equation 12 is restricting the latent distribution for the expert to a fixed Gaussian distribution $p_{\text{model}}(z)$ and maximizing the KL distance between the generated samples and the same fixed Gaussian distribution. More training details and full results, see in Appendix A.6.

Table 3 shows our VAE-based variant gets 8.1% and 34.8% relative improvement compared to the best baseline FAIRL and PWIL on clean and noisy expert data, respectively. This means that our VAE-based variant improves the imitation performance considerably compared to other baselines. It justifies that our AEAIL is flexible with different auto-encoders.

Question 4. *How our AEAIL performs with varying hidden size of the AE?*

To justify that our AEAIL is not sensitive to different sizes of the auto-encoder, we conduct ablations with different hidden sizes of AE.

Figure 5 shows the overall scaled rewards for AEAIL with different hidden sizes of AE. They achieve comparable results indeed. It depicts that our AEAIL is not sensitive to the size of AE while the hidden size of AE cannot be too small.

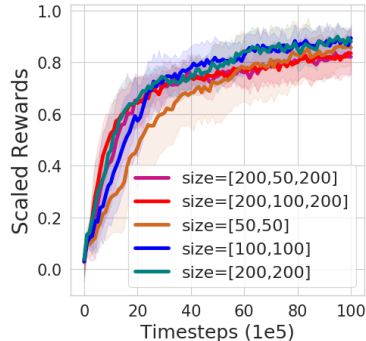


Figure 5: Training curve with scaled rewards overall.

6 Conclusions

This paper presents a straightforward and robust adversarial imitation learning method based on auto-encoding (AEAIL). We utilize the reconstruction error of an auto-encoder as the surrogate pseudo-reward function for reinforcement learning. The advantage is that the auto-encoder based reward function focused on the full-scale differences between the expert and generated samples, which provides a denser reward signal to the agent. As a result, it enables the agents to learn better. Experimental results show that our methods achieve strong competitive performances on both clean and noisy expert data. In the future, we want to further investigate our approach in more realistic scenarios, such as autonomous driving and robotics.

7 Boarder Impact

For potential positive impact, our proposed method AEAIL can better mimic the expert behaviors by learning from both clean and noisy demonstrations. It can help us to train a series of automation tools such as robots, navigation systems, self driving cars. However, for negative impact, teaching machines are cheaper than teaching and hiring human. It may results in unemployment in our society.

Acknowledgments and Disclosure of Funding

This work is supported by the Ministry of Science and Technology of the People’s Republic of China, the 2030 Innovation Megaprojects “Program on New Generation Artificial Intelligence” (Grant No. 2021AAA0150000).

References

- [1] Pieter Abbeel, Adam Coates, Timothy Hunter, and Andrew Y. Ng. Autonomous autorotation of an rc helicopter. In *International Symposium on Robotics*, 2008.
- [2] Pieter Abbeel, Adam Coates, and Andrew Y. Ng. Autonomous helicopter aerobatics through apprenticeship learning. *The International Journal of Robotics Research*, 2010.
- [3] Pieter Abbeel, Adam Coates, Morgan Quigley, and Andrew Y. Ng. An application of reinforcement learning to aerobatic helicopter flight. In *Advances in Neural Information Processing Systems (NeurIPS)*, 2007.
- [4] Pieter Abbeel, Dmitri Dolov, Andrew Y. Ng, and Sebastian Thrun. Apprenticeship learning for motion planning with application to parking lot navigation. In *IEEE/RSJ International Conference on Intelligent Robots and Systems*, 2008.
- [5] Pieter Abbeel, Varun Ganapathi, and Andrew Y. Ng. A learning vehicular dynamics, with application to modeling helicopters. In *Advances in Neural Information Processing Systems (NeurIPS)*, 2006.
- [6] Martin Arjovsky, Soumith Chintala, and Leon Bottou. Wasserstein gan. In *International Conference on Machine Learning (ICML)*, 2017.
- [7] Enda Barrett and Stephen Linder. Autonomous hva control, a reinforcement learning approach. *Machine Learning and Knowledge Discovery in Databases*, 2015.
- [8] Gabriel Barth-Maron, Matthew W Hoffman, David Budden, Will Dabney, Dan Horgan, Dhruva Tb, Alistair Muldal, Nicolas Heess, and Timothy Lillicrap. Distributed distributional deterministic policy gradients. *arXiv preprint arXiv:1804.08617*, 2018.
- [9] Glen Berseth and Christopher Pal. Visual imitation with reinforcement learning using recurrent siamese networks. 2020.
- [10] David Berthelot, Thomas Schumm, and Luke Metz. Began: Boundary equilibrium generative adversarial networks. In *Advances in Neural Information Processing Systems (NeurIPS)*, 2017.
- [11] Abdeslam Boularias, Jens Kober, and Jan Peters. Relative entropy inverse reinforcement learning. In *Proceedings of the Fourteenth International Conference on Artificial Intelligence and Statistics*, pages 182–189. JMLR Workshop and Conference Proceedings, 2011.
- [12] Daniel Brown, Wonjoon Goo, Prabhat Nagarajan, and Scott Niekum. Extrapolating beyond sub-optimal demonstrations via inverse reinforcement learning from observations. In *International Conference on Machine Learning (ICML)*, pages 783–792. PMLR, 2019.
- [13] Paul Christiano, Zain Shah, Igor Mordatch, Jonas Schneider, Trevor Blackwell, Joshua Tobin, Pieter Abbeel, and Wojciech Zaremba. Transfer from simulation to real world through learning deep inverse dynamics model. 2016.
- [14] Adam Coates, Pieter Abbeel, and Andrew Y. Ng. Learning for control from multiple demonstrations. In *International Conference on Machine Learning (ICML)*, 2008.
- [15] Robert Dadashi, Leonard Hussenot, Matthieu Geist, and Olivier Pietquin. Primal wasserstein imitation learning. In *International Conference on Learning Representations (ICLR)*, 2021.
- [16] Prafulla Dhariwal, Christopher Hesse, Oleg Klimov, Alex Nichol, Matthias Plappert, Alec Radford, John Schulman, Szymon Sidor, Yuhuai Wu, and Peter Zhokhov. Openai baselines, 2017.
- [17] Justin Fu, Katie Luo, and Sergey Levine. Learning robust rewards with adversarial inverse reinforcement learning. *International Conference on Learning Representations (ICLR)*, 2017.
- [18] Tanmay Gangwani and Jian Peng. State-only imitation with transition dynamics mismatch. In *International Conference on Learning Representations (ICLR)*, 2020.

- [19] Seyed Ghasemipour, Kamyar Seyed, Richard Zemel, and Shixiang Gu. A divergence minimization perspective on imitation learning methods. In *Conference on Robot Learning (CoRL)*, pages 1259–1277. PMLR, 2020.
- [20] Ian Goodfellow, Yoshua Bengio, and Aaron Courville. *Deep Learning*. MIT Press, 2016.
- [21] Ian J. Goodfellow, Jean Pouget-Abadie, Mehdi Mirza, Bing Xu, David Warde-Farley, Sherjil Ozair, Aaron Courville, and Yoshua Bengio. Generative adversarial nets. In *Advances in Neural Information Processing Systems (NeurIPS)*, 2014.
- [22] Daniel H Grollman and Aude G Billard. Robot learning from failed demonstrations. *International Journal of Social Robotics*, 4(4):331–342, 2012.
- [23] Ziwei Guan, Tengyu Xu, and Yingbin Liang. When will generative adversarial imitation learning algorithms attain global convergence. In *International Conference on Artificial Intelligence and Statistics (AISTATS)*, pages 1117–1125. PMLR, 2021.
- [24] Nicolas Heess, Gregory Wayne, David Silver, Timothy Lillicrap, Tom Erez, and Yuval Tassa. Learning continuous control policies by stochastic value gradients. In *Advances in Neural Information Processing Systems (NeurIPS)*, pages 2944–2952, 2015.
- [25] Jonathan Ho and Stefano Ermon. Generative adversarial imitation learning. In *Advances in Neural Information Processing Systems (NeurIPS)*, 2016.
- [26] Yujing Hu, Weixun Wang, Hangtian Jia, Yixiang Wang, Yingfeng Chen, Jianye Hao, Feng Wu, and Changjie Fan. Learning to utilize shaping rewards: A new approach of reward shaping. In *Advances in Neural Information Processing Systems (NeurIPS)*, 2020.
- [27] Mingxuan Jing, Xiaojian Ma, Wenbing Huang, Fuchun Sun, Chao Yang, Bin Fang, and Huaping Liu. Reinforcement learning from imperfect demonstrations under soft expert guidance. In *Proceedings of the AAAI Conference on Artificial Intelligence*, volume 34, pages 5109–5116, 2020.
- [28] Kuno Kim, Yihong Gu, Jiaming Song, Shengjia Zhao, and Stefano Ermon. Domain adaptive imitation learning. In *International Conference on Machine Learning (ICML)*, pages 5286–5295. PMLR, 2020.
- [29] Diederik P Kingma and Max Welling. Auto-encoding variational bayes. In *Advances in Neural Information Processing Systems (NeurIPS)*, 2014.
- [30] Edouard Klein, Bilal Piot, Matthieu Geist, and Olivier Pietquin. A cascaded supervised learning approach to inverse reinforcement learning. In *Joint European conference on machine learning and knowledge discovery in databases*, pages 1–16. Springer, 2013.
- [31] Ilya Kostrikov, Kumar Krishna Agrawal, Debidatta Dwibedi, Sergey Levine, and Jonathan Tompson. Discriminator-actor-critic: Addressing sample inefficiency and reward bias in adversarial imitation learning. In *International Conference on Learning Representations (ICLR)*, 2019.
- [32] Anders Boesen Lindbo Larsen, Søren Kaae Sønderby, Hugo Larochelle, and Ole Winther. Autoencoding beyond pixels using a learned similarity metric. In *International Conference on Machine Learning (ICML)*, 2016.
- [33] Sergey Levine and Vladlen Koltun. Guided policy search. In *International Conference on Machine Learning (ICML)*, pages 1–9, 2013.
- [34] Andrew Y. Ng, Adam Coates, Mark Diel, Varun Ganapathi, Jamie Schulte, Ben Tse, Eric Berger, and Eric Liang. Inverted autonomous helicopter flight via reinforcement learning. In *International Symposium on Experimental Robotics*, 2004.
- [35] Andrew Y Ng, Daishi Harada, and Stuart Russell. Policy invariance under reward transformations: Theory and application to reward shaping. In *International Conference on Machine Learning (ICML)*, 1999.
- [36] Manu Orsini, Anton Raichuk, Léonard Hussenot, Damien Vincent, Robert Dadashi, Sertan Girgin, Matthieu Geist, Olivier Frederic Bachem, Olivier Pietquin, and Marcin Andrychowicz. What matters for adversarial imitation learning? 2021.
- [37] Bilal Piot, Matthieu Geist, and Olivier Pietquin. Bridging the gap between imitation learning and inverse reinforcement learning. *IEEE transactions on neural networks and learning systems*, 28(8):1814–1826, 2016.

- [38] Ahmed H. Qureshi, Byron Boots, and Michael C. Yip. Adversarial imitation via variational inverse reinforcement learning. In *International Conference on Learning Representations (ICLR)*, 2019.
- [39] Nathan D. Ratliff, J. Andrew Bagnell, and Martin A. Zinkevich. Maximum margin planning. In *International Conference on Machine Learning (ICML)*, 2006.
- [40] John Schulman, Sergey Levine, Pieter Abbeel, Michael Jordan, and Philipp Moritz. Trust region policy optimization. In *International Conference on Machine Learning (ICML)*, pages 1889–1897. PMLR, 2015.
- [41] John Schulman, Philipp Moritz, Sergey Levine, Michael Jordan, and Pieter Abbeel. High-dimensional continuous control using generalized advantage estimation. In *International Conference on Learning Representations (ICLR)*, 2016.
- [42] Kyriacos Shiarlis, Joao Messias, and Shimon Whiteson. Inverse reinforcement learning from failure. In *Proceedings of the 2016 International Conference on Autonomous Agents & Multiagent Systems (AAMAS)*, pages 1060–1068, 2016.
- [43] Bradley C. Stadie, Pieter Abbeel, and Ilya Sutskever. Third-person imitation learning. In *International Conference on Learning Representations (ICLR)*, 2017.
- [44] Yuval Tassa, Tom Erez, and Emanuel Todorov. Synthesis and stabilization of complex behaviors through online trajectory optimization. In *2012 IEEE/RSJ International Conference on Intelligent Robots and Systems*, pages 4906–4913. IEEE, 2012.
- [45] David Warde-Farley and Yoshua Bengio. Improving generative adversarial networks with denoising feature matching. In *International Conference on Learning Representations (ICLR)*, 2017.
- [46] Yueh-Hua Wu, Nontawat Charoenphakdee, Han Bao, Voot Tangkaratt, and Masashi Sugiyama. Imitation learning from imperfect demonstration. In *Proceedings of the 36th International Conference on Machine Learning (ICML)*, pages 6818–6827, 2019.
- [47] Xin Zhang, Yanhua Li, Ziming Zhang, and Zhi-Li Zhang. f-gail: Learning f-divergence for generative adversarial imitation learning. *Advances in Neural Information Processing Systems (NeurIPS)*, 33, 2020.
- [48] Junbo Zhao, Machael Mathieu, and Yann LeCun. Energy-based generative adversarial network. *International Conference on Learning Representations (ICLR)*, 2016.
- [49] Brian D. Ziebart, J. Andrew Bagnell, and Anind K. Dey. Modeling interaction via the principle of maximum causal entropy. In *International Conference on Machine Learning (ICML)*, 2010.
- [50] Brian D. Ziebart, Andrew Maas, J. Andrew Bagnell, and Anind K. Dey. Maximum entropy inverse reinforcement learning. In *AAAI Conference on Artificial Intelligence (AAAI)*, 2008.

Checklist

1. For all authors...
 - (a) Do the main claims made in the abstract and introduction accurately reflect the paper’s contributions and scope? [\[Yes\]](#)
 - (b) Did you describe the limitations of your work? [\[Yes\]](#) See in Section 7
 - (c) Did you discuss any potential negative societal impacts of your work? [\[Yes\]](#) See in Section 7
 - (d) Have you read the ethics review guidelines and ensured that your paper conforms to them? [\[Yes\]](#)
2. If you are including theoretical results...
 - (a) Did you state the full set of assumptions of all theoretical results? [\[Yes\]](#) See in Section 4.3
 - (b) Did you include complete proofs of all theoretical results? [\[N/A\]](#)
3. If you ran experiments...
 - (a) Did you include the code, data, and instructions needed to reproduce the main experimental results (either in the supplemental material or as a URL)? [\[Yes\]](#) code and data see in supplementary materials, instructions see in Appendix A.2

- (b) Did you specify all the training details (e.g., data splits, hyperparameters, how they were chosen)? [Yes] see in Appendix A.2
 - (c) Did you report error bars (e.g., with respect to the random seed after running experiments multiple times)? [Yes]
 - (d) Did you include the total amount of compute and the type of resources used (e.g., type of GPUs, internal cluster, or cloud provider)? [Yes] see in Appendix A.2
4. If you are using existing assets (e.g., code, data, models) or curating/releasing new assets...
- (a) If your work uses existing assets, did you cite the creators? [Yes] we builds our method based on OpenAI baselines
 - (b) Did you mention the license of the assets? [Yes] see in Appendix A.2, we use an open source MuJoCo license for experiments.
 - (c) Did you include any new assets either in the supplemental material or as a URL? [N/A]
 - (d) Did you discuss whether and how consent was obtained from people whose data you're using/curating? [N/A]
 - (e) Did you discuss whether the data you are using/curating contains personally identifiable information or offensive content? [N/A]
5. If you used crowdsourcing or conducted research with human subjects...
- (a) Did you include the full text of instructions given to participants and screenshots, if applicable? [N/A]
 - (b) Did you describe any potential participant risks, with links to Institutional Review Board (IRB) approvals, if applicable? [N/A]
 - (c) Did you include the estimated hourly wage paid to participants and the total amount spent on participant compensation? [N/A]

A Appendix

A.1 Pseudo code

Algorithm 1 Auto-Encoding Adversarial Imitation Learning (AEAIL)

Input: Initial parameters of policy, auto-encoder θ_0, w_0 ; Expert trajectories D_E .

repeat

Sample state-action pairs $(s_i, a_i) \sim \pi_{\theta_i}$ and $(s_E, a_E) \sim D_E$ with same batch size.

Update w_i to w_{i+1} by decreasing with the gradient:

$$\mathbb{E}_{(s_i, a_i)}[\nabla_{w_i} 1/(1 + \text{AE}_{w_i}(s_i, a_i))] - \mathbb{E}_{(s_E, a_E)}[\nabla_{w_i} 1/(1 + \text{AE}_{w_i}(s, a))]$$

Take a policy step from θ_i to θ_{i+1} , using the TRPO update rule with the reward function $1/(1 + \text{AE}_{w_i}(s, a))$, and the objective function for TRPO is:

$$\mathbb{E}_{(s, a)}[-1/(1 + \text{AE}_{w_i}(s, a))].$$

until π_{θ} converges

Algorithm 1 depicts the pseudo-code for training AEAIL. The first step is to sample the state-action pairs from expert demonstrations D_E and the trajectories sampled by the current policy with the same batch size. Then we update the auto-encoder by decreasing with the gradient with loss function Eq. 9. Finally, we update the policy assuming that the reward function is Eq. 7 which leads to an adversarial training paradigm. We repeat these steps until the approach converges.

A.2 Implementation

Data, code, and video see in project website <https://sites.google.com/view/auto-encoding-imitation>. This section will introduce the implementation details, including tasks, basic settings for all algorithms, baseline implementations, network architecture for our approach.

A.2.1 Tasks

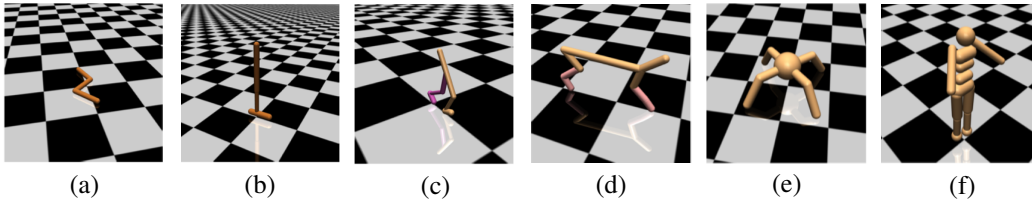


Figure 6: Illustrations for locomotion tasks we used in our experiments: (a) Swimmer; (b) Hopper; (c) Walker; (d) HalfCheetah; (e) Ant; (f) Humanoid.

The goal for all these tasks is to move forward as quickly as possible. These tasks are more challenging than basic ones due to high degrees of freedom. In addition, a great amount of exploration is needed to learn to move forward without getting stuck at local optima. Since we penalize for excessive controls and falling over, during the initial stage of learning, when the robot cannot move forward for a sufficient distance without falling, apparent local optima exist, including staying at the origin or moving forward slowly. Figure 6 depicts locomotion tasks' environments.

A.2.2 Resources and License

We use 8 GTX 3080 GPU and 40 CPU to run the experiments. Our algorithm needs ~ 40 hours for training on 6 tasks with 5 random seeds. We also use an open source MuJoCo license to run the locomotion tasks. The license can be found here: <https://mujoco.org>.

A.2.3 Basic settings

We sample the expert trajectories with PPO on Walker2d, Hopper, Swimmer, HalfCheetah, and Ant with 25 trajectories. We sample 320 trajectories on Humanoid with SAC to get higher expert performance since PPO is not good enough on Humanoid.

We normalize the state features for each task and use the normalized features as the input for the auto-encoder. We also use the raw data input to compute the final output of the mean square error.

We train these algorithms directly on Walker2d, Hopper, and Swimmer, while on HalfCheetah, Ant, and Humanoid, we use BC to pre-train the policy with 10k iterations. We test all the algorithms on these six locomotion tasks with five random seeds and using ten rollouts to estimate the ground truth rewards to plot the training curves.

The maximum length for sampled trajectories is 1024. The discounted factor is 0.995. Each iteration, we update three times of policies and one time of the reward function (discriminator or auto-encoder). While updating TRPO, we update the critic five times with a learning rate of $2e-4$ every iteration.

A.2.4 Baselines

We use open-source code, OpenAI baselines [16], to get the performance of BC, and the training iterations is 100k for all tasks.

GAIL [25] borrows the GAN [21] architecture to realize the IRL process, and it is applicable in high dimensional dynamic environments. We implement GAIL with open-source code, OpenAI baselines [16], with best tuned hyperparameters. We choose TRPO as the reinforcement learning algorithm for a fair comparison.

WGAIL [6, 25] utilizes the Wasserstein distance to train the policy and the reward function, which can be more stable. WGAIL is implemented based on GAIL with W-distance based objective function as in [6]. We also choose TRPO as the reinforcement learning algorithm for a fair comparison. More specifically, the objective function for WGAIL is:

$$\mathcal{L} = \min_{\pi_{\theta}} \max_{r_w} \mathbb{E}_{(s,a) \sim D_E} [r_w(s, a)] - \mathbb{E}_{(s,a) \sim \pi_{\theta}} [r_w(s, a)], \quad (13)$$

where $r_w(s, a) = D(s, a)$ and the discriminator D is formulated with a discriminator. We don't add Lipschitz constraint to the objective since we restrict the function to class of neural networks. Incidentally, [36] introduces that whether using regularization or not doesn't have much efforts for AIL methods.

FAIRL [19] utilizes the forward KL divergence as the objective, which shows competitive performances on MuJoCo tasks. FAIRL is implemented based on GAIL with corresponding objective function as in [19]. We also choose TRPO as the reinforcement learning algorithm for a fair comparison.

PWIL [15] is an imitation learning method based on an offline similarity reward function. It is pretty robust and easy to fine-tune the hyper-parameters of its reward function (only two hyper-parameters). PWIL is implemented based on open source code [15] with TRPO as the reinforcement learning method for a fair comparison (original PWIL code uses D4PG as the RL algorithm).

A.2.5 Architecture of our methods

Policy Net: two hidden layers with 64 units, with tanh nonlinearities in between, which is the same with baselines. The learning rate we used for updating the policy is 0.01.

Auto-Encoder Net: (both vanilla auto-encoder and variational auto-encoder) the number of layers is the same with the architecture of discriminator in GAIL, i.e., four layers. The two hidden layers are with 100 units, with tanh nonlinearities in between, the final output layer is an identity layer. We normalize the state feature after the input layer, and we use the raw state action input features to compute the mean square error. The learning rate for the auto-encoder is $3e-4$.

A.3 Training curves on noisy expert demonstrations

We conduct experiments on noisy expert demonstrations in Section 5.2. The noise component is a Gaussian distribution noise which is $(0, 0.3)$ for Walker2d, Hopper, Swimmer, HalfCheetah. Since

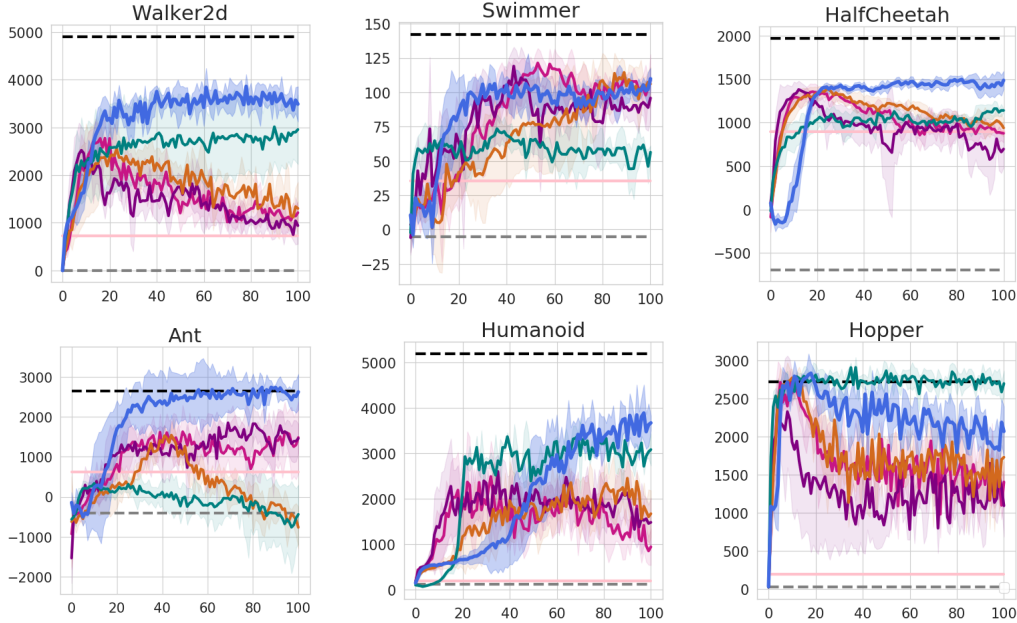


Figure 7: Mean and standard deviation return of the evaluation policy over 10 rollouts and 5 seeds learning from noisy expert demonstrations, reported every 100k timesteps. The legend is the same with Figure 2 while the **blue** line represents ours.

Table 4: Learned policy performance for different imitation learning algorithms on another noise magnitude.

Task	Walker2d	Hopper	Swimmer	HalfCheetah	Ant	Humanoid
GAIL	913 \pm 175	489 \pm 98	77 \pm 13	248 \pm 32	1021 \pm 764	765 \pm 353
WGAIL	664 \pm 246	828 \pm 313	65 \pm 11	259 \pm 129	1032 \pm 373	943 \pm 468
FAIRL	952 \pm 433	1003 \pm 384	84 \pm 9	342 \pm 67	-1488 \pm 764	1243 \pm 479
PWIL	2095 \pm 564	2570 \pm 145	49 \pm 6	563 \pm 54	-1567 \pm 864	2793 \pm 286
Ours	2141 \pm 232	1392 \pm 217	94 \pm 7	1082 \pm 67	1644 \pm 345	3024 \pm 126

the effects of the noise component perform more heavily on Ant and Humanoid, we choose $(0, 0.03)$ and $(0, 0.01)$ Gaussian distribution noise for Ant and Humanoid, respectively. Under these settings, higher final ground truth rewards indicate better robustness of its corresponding algorithm.

Figure 7 shows the training curves for different imitation learning algorithms on the noisy expert demonstrations. On Walker2d, Swimmer, HalfCheetah, Ant, and Humanoid, our AEAIL outperforms other baselines. However, on Hopper, PWIL achieves the best performance.

We scale the ground truth rewards of final policy performance for different methods, which considers the expert trajectory’s rewards as 1 and random policy trajectory’s rewards as 0. The average scaled ground truth reward is 0.794 for our method while the best baseline is 0.539 for PWIL. We achieve 47.2% relative improvement overall compared to PWIL. In summary, our method is much more robust to the noisy expert than other baselines.

For more convincing results, we also conduct experiments with another noise magnitude. For Walker2d, Hopper, Swimmer and HalfCheetah, we add a Gaussian $(0, 0.5)$ to each dimension of the expert data pair. And for Ant, we add a Gaussian noise $(0, 0.05)$ to the expert data pair. For Humanoid task, we add a Gaussian noise $(0, 0.03)$ to the expert data pair.

Table 4 shows that our AEAIL is consistently better than other baselines overall on different noise magnitude.

A.4 Analysis on t-SNE visualization results

AIL methods recover the expert policy through confusing the reward signal with maximizing the total episode rewards. Consequently, the final policy generated samples and expert samples would demonstrate identical distribution. t-SNE help us to visualize the low dimensional representations of high dimensional samples. In this section, we will visualize the latent representations of reward functions between expert and generated samples. The latent representations for policy-generated samples and expert samples will be greatly overlapped if imitation learning works well. The overlapping areas also reflects the robustness of their agent policies, when confronted with the noisy experts. Since PWIL [15] considers a hand-crafted reward function without neural networks, we only compare our methods with the other three baselines.

Table 5: Hyper-parameters for t-SNE visualization

Hyper-parameter	Value
n_component	2
early_exaggeration	float 12.0
learning_rate	200.0
n_iter	int 1000
n_iter_without_progress	int 300
min_grad_norm	float 1e-7
metric	'euclidean'
init	'pca'

For the discriminator-based methods, we visualize the output of the first hidden (middle) layer. For our auto-encoder based reward function, we visualize the output of the first hidden (middle) layer in the net. We plot the t-SNE embedding results with the scikit-learn library (i.e., sklearn.manifold.TSNE function) with varying perplexity. The hyper-parameters for t-SNE are (other hyper-parameters are default with scikit-learn) shown in Table 5.

Figure 8 depicts the two sets of samples in the latent space of the corresponding reward signals. Typically, perplexity = 30.0 is a common hyper-parameter for using t-SNE. But other choices of perplexity can also show the robustness of these methods.

With varying perplexity, we can observe the overlapping areas for policy and expert embeddings are always the greatest for our method compared to other baselines. Detailly with perplexity=30.0, considering non-noisy setting, we can observe that the policy samples for GAIL and WGAIL hardly appear in the outer ring. And FAIRL is a little better than GAIL and WGAIL. Our AEAIL gets maximum overlap between two sets of samples compared to these baselines. And under the noisy settings, the two sets of embeddings of GAIL and WGAIL are actually isolated while they are partly clustered for FAIRL. The embeddings are significantly overlapped for our method. As a result, it reflects that our method better mimics the expert behaviors on both clean and noisy expert data.

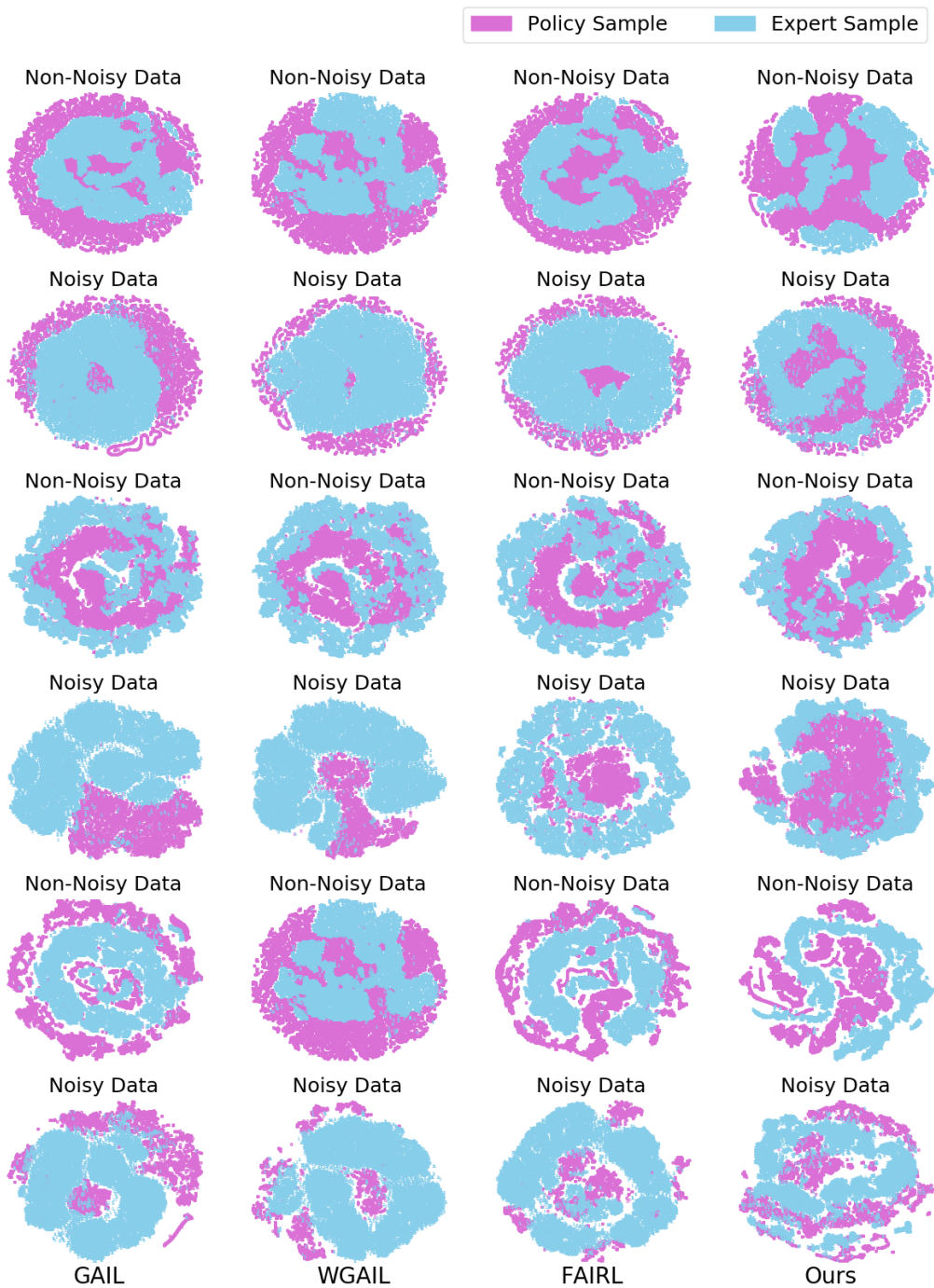


Figure 8: t-SNE visualization of latent representations of the reward function on Walker2d for different methods. Top two row: perplexity=5.0; Middle two row: perplexity=30.0; Bottom two row: perplexity=50.0. The noise component is a Gaussian $(0, 0.5)$.

A.5 Ablation study: different distribution divergences

We conduct an ablation study with Jensen-Shannon divergence. We run the experiments with a new form of reward function based on Jensen-Shannon divergence [21] for comparison.

Jensen-Shannon divergence is defined as:

$$\text{JS}(P_r, P_g) = \mathbb{E}_{x \sim P_r} \left[\log \left(\frac{P_r(x)}{\frac{1}{2}(P_r(x) + P_g(x))} \right) \right] + \mathbb{E}_{x \sim P_g} \left[\log \left(\frac{P_g(x)}{\frac{1}{2}(P_r(x) + P_g(x))} \right) \right], \quad (14)$$

where P_r and P_g represents the expert data distribution and the generated data distribution. The adversarial training procedure of AEAIL will match the state-action distribution of expert and generated samples.

In this form of reward function, we consider the exponential of negative reconstruction error as: $P_r(x)/(P_r(x) + P_g(x))$. The derived Jensen-Shannon divergence for updating the auto-encoder based reward function is:

$$\mathcal{L} = - \mathbb{E}_{(s,a) \sim D_E} [\log(\exp(-\text{AE}_w(s, a)))] - \mathbb{E}_{(s,a) \sim \pi} [\log(1 - \exp(-\text{AE}_w(s, a)))] \quad (15)$$

$$= \mathbb{E}_{(s,a) \sim D_E} [\text{AE}_w(s, a)] - \mathbb{E}_{(s,a) \sim \pi} [\log(1 - \exp(-\text{AE}_w(s, a)))] \quad (16)$$

Here, w represents the parameters of the auto-encoder network. Its formulation of surrogate reward function is:

$$r_w(s, a) = -\log(1 - \exp(-\text{AE}_w(s, a))). \quad (17)$$

Minimizing the Jensen-Shannon divergence between state-action distribution of the expert and generated trajectories assigns low mean square errors to the expert samples and high mean square errors to other regions. And intuitively, we give high rewards to the regions with low reconstruction errors and vice versa.

Table 6: Learned final policy performance for our AEAIL with W-distance (Ours) and JS-distance (Ours-JS) respectively. Top two rows: non-noisy expert; Bottom two rows: noisy expert.

Task	Walker2d	Hopper	Swimmer	HalfCheetah	Ant	Humanoid
Ours	3870 ± 196 [↑]	2621 ± 140 [↓]	143 ± 3 [↓]	1623 ± 52 [↓]	2846 ± 204 [↓]	4004 ± 570 [↑]
Ours-JS	3589 ± 427 [↓]	2771 ± 67 [↑]	143 ± 3 [↑]	1671 ± 20 [↑]	3063 ± 282 [↑]	2167 ± 1212 [↓]
Ours	3491 ± 369 [↓]	2072 ± 327 [↑]	110 ± 8 [↑]	1487 ± 105 [↑]	2622 ± 445 [↓]	3666 ± 155 [↑]
Ours-JS	3562 ± 346 [↑]	1672 ± 127 [↓]	106 ± 4 [↓]	1429 ± 40 [↓]	2675 ± 134 [↑]	2521 ± 861 [↓]

The results in Table 6 show that W-distance based method is comparable with JS-distance based method on almost all tasks. Our JS based variant achieves 10.6% and 35.1% relative improvement compared to the best baseline FAIRL and PWIL on clean and noisy expert data, respectively. It is similar to the W-distance based variant. This indicates that the encoding-decoding process is the major contributing factor in our AEAIL which improves the imitation performance rather than the specific distribution divergence.

A.6 Ablation study: utilizing other auto-encoders

We conduct experiments with variational auto-encoder based reward function as an ablation. The variational auto-encoder [29] is a directed model that uses learned approximate inference. The critical insight behind training variational auto-encoder is to maximize the variational lower bound $\mathcal{L}(q)$ of the log-likelihood for the training examples [20]:

$$\mathcal{L}(q) = \mathbb{E}_{z \sim q(z|x)} \log p_{\text{model}}(z, x) + \mathcal{H}(q(z|x)) \quad (18)$$

$$= \mathbb{E}_{z \sim q(z|x)} \log p_{\text{model}}(x|z) - D_{\text{KL}}(q(z|x) \| p_{\text{model}}(z)) \quad (19)$$

$$\leq \log p_{\text{model}}(x) \quad (20)$$

where z is the latent representation for data points x . And p_{model} is chosen to be a fixed Gaussian distribution $\mathcal{N}(0, I)$. Training the variational auto-encoder is still a adversarial process. We notice

that the first term in Eq. 19 is the reconstruction log-likelihood found in traditional auto-encoders. The objective function for training the variational auto-encoder is:

$$\begin{aligned} \mathcal{L} = & \mathbb{E}_{(s,a) \sim D_E} [r_w(s, a) + D_{\text{KL}}(p(z|(s, a)), p_{\text{model}}(z))] \\ & - \mathbb{E}_{(s,a) \sim \pi_\theta} [r_w(s, a) + D_{\text{KL}}(p(z|(s, a)), p_{\text{model}}(z))] \end{aligned} \quad (21)$$

where the choice for $r_w(s, a)$ is the same with our AE based one, which is Eq. 7 in Section 4.2. When minimizing this objective, the variational auto-encoder based reward function can still assign high values near the expert demonstrations and low values to other regions. On the other hand, optimizing this objective is restricting the latent distribution for the expert to a fixed Gaussian distribution $p_{\text{model}}(z)$ and maximizing the KL distance between the generated samples and the same fixed Gaussian distribution.

Table 7: Learned final policy performance for Our AE based variant (Ours) and VAE based variant (Ours-VAE) respectively. Top two rows: on non-noisy expert; Bottom two rows: on noisy expert.

Task	Walker2d	Hopper	Swimmer	HalfCheetah	Ant	Humanoid
Ours	3870 ± 196↓	2621 ± 140↓	143 ± 3↑	1623 ± 52↓	2846 ± 204↑	4004 ± 570↑
Ours-VAE	4013 ± 249↑	2851 ± 151↑	136 ± 6↓	1644 ± 11↑	2333 ± 938↓	2487 ± 1419↓
Ours	3491 ± 369↓	2072 ± 327↓	110 ± 8↑	1487 ± 105↑	2622 ± 445↑	3666 ± 155↑
Ours-VAE	4079 ± 295↑	2210 ± 108↑	88 ± 9↓	1335 ± 149↓	2401 ± 423↓	2159 ± 1001↓

Table 7 shows the results for our AE based variant and VAE based variant on both clean and noisy expert data. Our VAE based variant gets 8.1% and 34.8% relative improvement compared to the best baseline FAIRL and PWIL, respectively. Comprehensively, our AEAIL works well with the VAE formulation.

A.7 Additional experiments on better synthesis experts

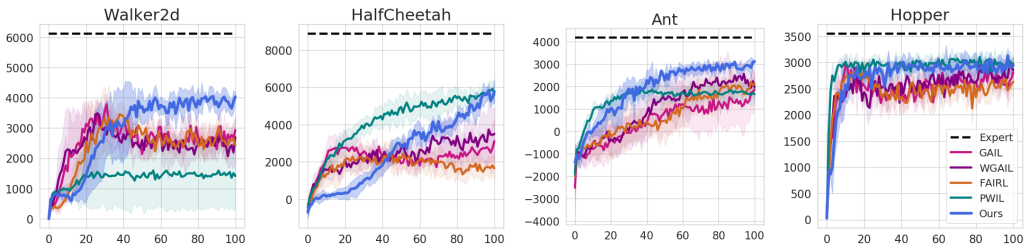


Figure 9: Mean and standard deviation return of the evaluation policy over 10 rollouts and 5 seeds, learning from **non-noisy** expert demonstrations, reported every 100k timesteps. The return is in term of the environment’s ground truth reward.

Table 8: Learned policy performance for different imitation learning algorithms on non-noisy expert data.

Task	Walker	Hopper	HalfCheetah	Ant
Expert	6121.7	3548.0	8879.1	4177.0
GAIL	2933.4 ± 392.6	2807.1 ± 196.1	3107.4 ± 1138.9	1866.9 ± 688.8
WGAIL	2692.5 ± 746.7	2850.3 ± 198.8	3502.2 ± 1411.0	1964.6 ± 575.1
FAIRL	2425.0 ± 216.2	2630.4 ± 263.8	1655.9 ± 591.6	2107.2 ± 324.7
PWIL	1414.8 ± 1033.8	2969.5 ± 86.7	5608.8 ± 411.0	1661.2 ± 397.8
Ours	4036.8 ± 159.8	2939.2 ± 183.4	5775.1 ± 644.8	3104.1 ± 95.4

To get more convincing results, we conduct experiments on better synthesis experts. We collect the expert demonstration with 16 trajectories for each task via D4PG [8]. Figure 9 depicts the training

curves of ground truth rewards for different algorithms. The training curve shows the imitation performance learning from non-noisy expert data. Table 8 shows the final learned policy performance on MuJoCo tasks with ground truth episode return. The overall results are similar to what we have gotten in the main text. On Walker2d, HalfCheetah, and Ant, our method gets the best performance. On Hopper, PWIL receives the best performance, and our AEAIL is on par with PWIL.

We take the random and expert samples as 0 and 1 respectively to compute the scaled rewards for different methods. The overall averaged scaled rewards for our method is about 0.729, while the best baseline is 0.546 for PWIL. There is an about 33.7% relative improvement overall.